

Noise analysis and reduction in full tensor gravity gradiometry data

Gary J. Barnes ¹ and John M. Lumley ²

¹ ARKeX Ltd, Cambridge, U.K. (gary.barnes@arkex.co.uk)

² ARKeX Ltd, Cambridge, U.K. (john.lumley@arkex.com)

Introduction

The Full Tensor Gradiometer (FTG) consists of three distinct modules known as gravity gradient instruments each measuring components of differential curvature. When one sums the three inline outputs to form a quantity known as the 'inline sum', the signals cancel leaving a residual that forms a useful estimate of the overall FTG performance. This quantity not only forms a useful quality control measure, but also gives insight into the level and colour (spectral shape) of the gradiometer noise.

When analysing survey data, the make-up of the noise can be partitioned into three categories, 1) shifts in the mean level, 2) correlated noise and 3) uncorrelated high frequency noise. The uncorrelated noise is generally what is left over after software corrections that reduce the interference from the linear and angular motions of the aircraft. Apart from filtering and averaging, little can be done to reduce this part of the noise. Shifts in the mean level can be seen when viewing data from line to line where data levels typically shift during the survey turns where different operating conditions exist and the instrument (being on a stabilised platform) acquires a new attitude in the aircraft. Correlated noise can be caused by environmental changes such as temperature and pressure and is evident when studying power spectral densities of the inline sum at low frequency. Figure 1 shows the power spectral density of the inline sum divided by $\sqrt{3}$ to give the average noise per FTG output during a typical survey.

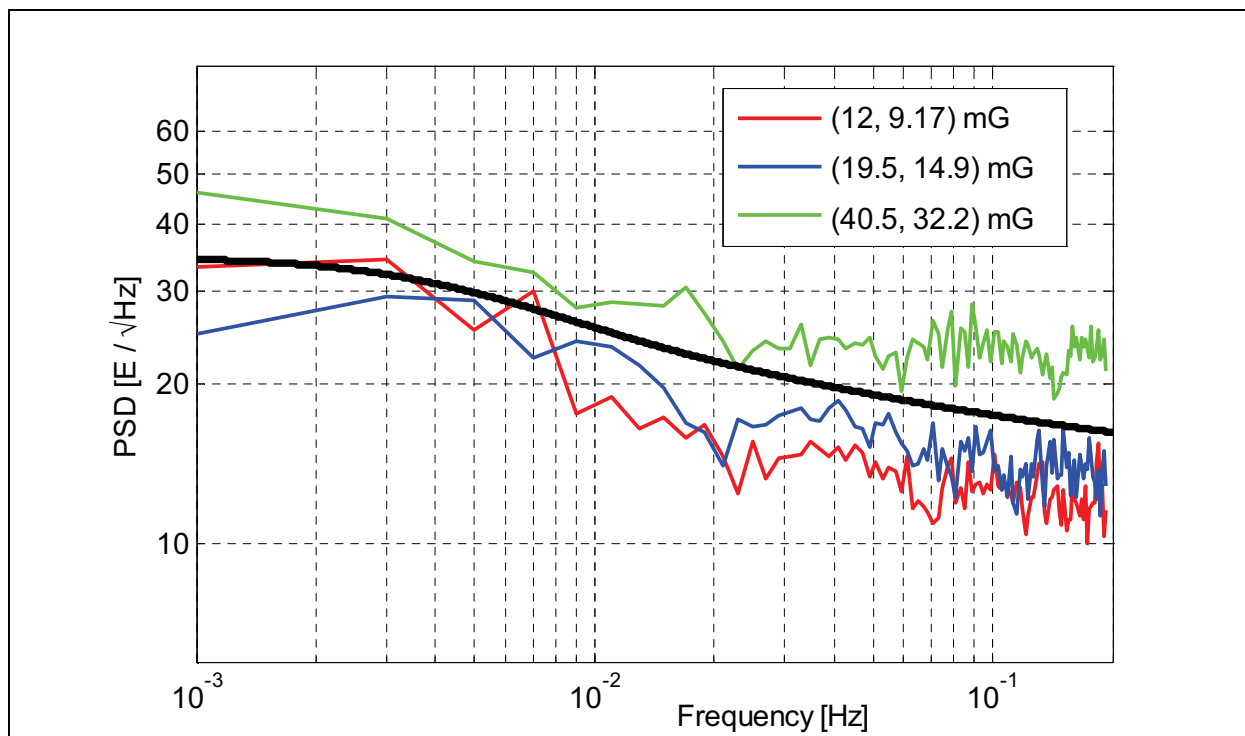


Figure 1. FTG output channel noise from ARKeX survey data for 3 levels of turbulence as shown in the legend quantified as (mean level, median level of vertical acceleration power over a 5 second window). Black line shows an empirical noise model fitted to the data.

The data used in this analysis consisted of approximately 250 survey lines that had been accepted by quality control measures which generally discard lines flown in excessive turbulence. Further details of the analysis of FTG noise as a function of turbulence can be found in Barnes et al., (2010). Some of the increase in low frequency power in this measure derives from real signal power leaking into the inline sum measure. The cancellation of the signal is particularly sensitive to the precise calibration of the FTG output channels and unless test lines flown at high altitude are used, the noise power at low frequency will tend to be over-estimated. Nevertheless, the red nature of the spectrum does indicate the presence of correlated noise in the data and to recover the best estimates of the signal, this must be addressed in the processing strategies.

Low frequency noise or drift is normally handled by levelling procedures that, given an adequate number of survey line – tie line intersection points, can correct the mean levels together with low order trends in the data. However, when airborne FTG surveys are flown in a manner where they loosely follow terrain, also known as ‘2-D drape’, the horizontal intersection points between survey and tie lines can have large differences in height. In these situations, standard levelling methods become compromised since they cannot rely on the signal at the intersection points being equal.

To resolve this problem, we use a modification to the equivalent source method that encompasses a time domain drift model (Barnes, 2008). The variation of the signal with height is then accommodated by the spatial equivalent source model whereas the mean level and low order drift is handled by a separate time domain part. After the inversion, the correlated noise absorbed by the time domain part of the model is discarded leaving an equivalent source model that can be used to forward calculate data free from the mean level shifts and much of the drift. Such a technique has been used successfully for surveys performed in mountainous regions where the height difference between survey and tie lines can be several hundreds of metres.

Method

To model the drift, a simple time interpolation function can be constructed by stringing together piece-wise linear sections at regular intervals (Figure 2).

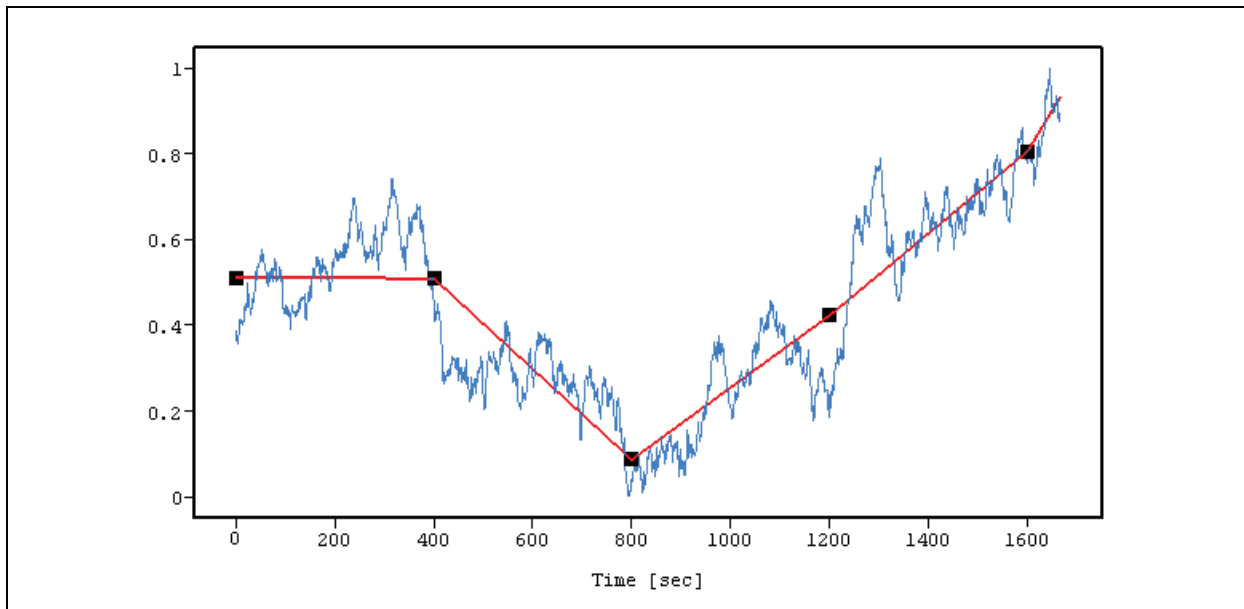


Figure 2. Exponentially correlated noise time series with a 500 second characteristic time (blue series) modelled by a piece-wise linear interpolator (red series) with nodal points every 400 seconds (black squares).

The model is entirely specified by the values at the nodal points, v_j , therefore making the number of degrees of freedom equal to the number of nodal points. Collecting these nodal values in a vector \mathbf{v} , the drift values \mathbf{d} at the time instants of the measurements can be expressed as a matrix equation,

$$\mathbf{d} = \mathbf{B} \mathbf{v} \quad (1)$$

where \mathbf{B} is a matrix that defines the interpolation. To understand how (1) works, consider the i th measurement whose acquisition time t_i falls between nodal drift values j and $j+1$ defined at times t_j and t_{j+1} . The linear interpolated value at time t_i is given by

$$d_i = \left(\frac{t_i - t_j}{t_{j+1} - t_j} \right) v_j + \left(1 - \frac{t_i - t_j}{t_{j+1} - t_j} \right) v_{j+1}. \quad (2)$$

The two terms in brackets represent the matrix elements $B_{i,j}$ and $B_{i,j+1}$.

For most airborne gradiometer surveys with lines of duration less than 30 minutes, there is insufficient time for complex drift variations to occur and a single linear trend or just simply a bias term encompassing an entire survey line often suffices.

The space domain part of the inversion follows a standard equivalent source method where the densities of discrete elements of a model are deduced so that forward calculations from the model fit the measurements in a least squares sense. The discretisation takes the form of a grid of rectangular prisms having a top surface following the terrain and a horizontal bottom surface placed below the minimum point in the topography. This construction therefore naturally builds in the upward continuation effect in an airborne survey and consequently makes the inversion more immune to high frequency noise in the data. Having a fixed geometry and solving for the density distributions makes the inversion linear and suitable for a variety of solvers such as the conjugate gradient algorithm (Press et al., 1997).

One of the biggest shortcomings of the equivalent source method regards its efficiency. To construct the inversion one needs to populate a matrix \mathbf{A} that represents the unit density forward calculations from each element in the model to each measurement in the data set. Multiplying this matrix with the density vector $\boldsymbol{\rho}$ then gives the signals, \mathbf{f}_s , predicted from the model,

$$\mathbf{f}_s = \mathbf{A} \boldsymbol{\rho} \quad (3).$$

The problem here is that the matrix \mathbf{A} is fully populated and extremely large for typical surveys. To honour the high bandwidth of gradient data, the measurements cannot be heavily re-sampled to reduce data volume, and similarly, the design of the equivalent source model must be of sufficiently high resolution.

To make the formulation practicable, we assert that blocks of the model which are distant from the field point can be grouped together to form a larger averaged block. The averaged block has a top surface, bottom surface and density all being the average of the individual blocks that it encompasses. Being distant, this is a valid approximation since the finer details of a field diminish rapidly with distance from the source. Parts of the model close to the field point are not grouped together thus preserving their short wavelength contributions to the field. An algorithm decides how to group the elements using a recursive quadtree subdivision process that starts off with the biggest averaged block of all – one that encompasses the entire model grid. This block is then subdivided into 4 smaller sized blocks if its size (defined by the longest x-y dimension) is greater than some factor l multiplied by the x-y distance between the centre of the block and the field point,

$$\text{subdivide if } \text{Max}(L_x, L_y) > l \sqrt{(x_c - x_f)^2 + (y_c - y_f)^2} \quad (4)$$

where L_x and L_y are the block dimensions, (x_c, y_c) is the centre of the block and (x_f, y_f) is the field point. The factor l controls the level of approximation, where a value of zero would resort back to

the full calculation with no grouping (i.e., subdivide at every step) and a value of one is generally a crude approximation.

Figure 3 demonstrates the accuracy of the approximation by evaluating a forward calculation along a survey line with l values of 0 (representing the exact answer), and 1.5 (representing a crude approximation level). Even though the error in the approximation level when l was equal to 1.5 is small compared to the noise in FTG data, it is not necessarily a random variable. Consequently, more conservative approximation factors for l (e.g., 0.3) are often used for the inversions to ensure accurate results (note: the result for this value of l is not shown in Figure 3 as it lies within the line width of the exact answer). By utilising this scheme, the matrix \mathbf{A} can be represented as a sparse matrix with occupancy typically around 1% and therefore offering considerable memory saving and efficient solution times.

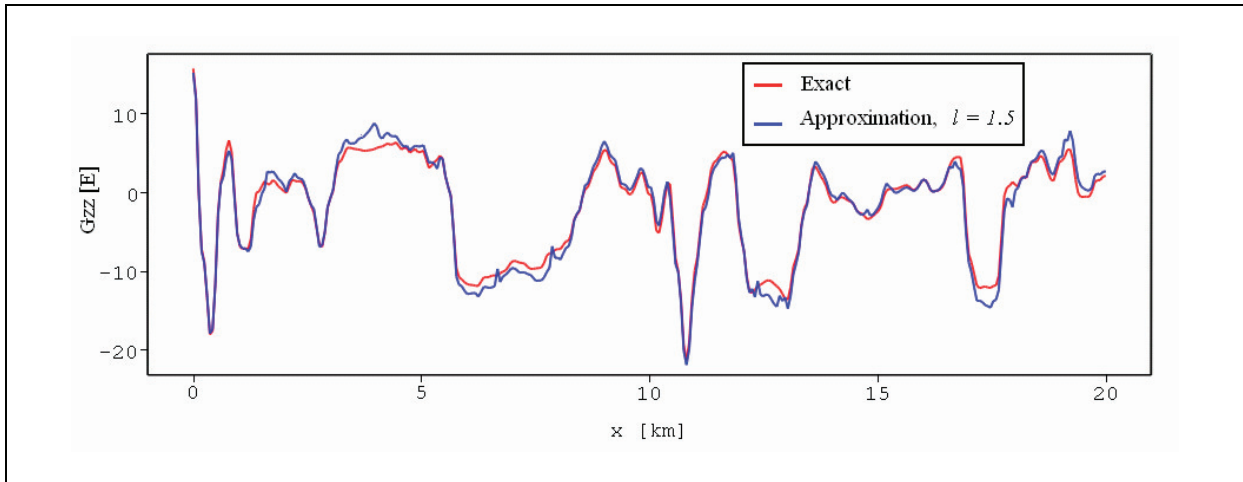


Figure 3. Comparison of full forward calculation (red) and approximate method (blue). The full calculation required 3.1×10^6 function evaluations, whilst the approximate calculation required only 7900 evaluations. The standard deviation of the differences indicated that the approximation had an accuracy of 0.6 E.

The time domain drift and space domain equivalent source terms are combined together to form a single optimisation problem where the density vector \mathbf{p} and the drift vector \mathbf{v} are solved for simultaneously,

$$\text{minimise } \left\{ (\mathbf{A}\mathbf{p}(x, y, z) + \mathbf{B}\mathbf{v}(t) - \mathbf{m}(x, y, z, t))^2 \right\} \quad (5).$$

where $\mathbf{m}(x, y, z, t)$ represent the measurements. These types of inversion problems invariably require regularisation to stabilise the solution. In this case adding a regularisation term to prefer smooth solutions to the density distribution makes sense since the fields from the Earth tend to be spatially correlated (deGroot-Hedlin and Constable, 1990). Regularisation of this type aids in the correct assignment between signal and drift as well as improving the robustness of the inversion and the spatial continuity of the equivalent source model between measurement locations. The drift is correlated in the time domain whilst the signal is correlated in the space domain. By favouring a spatially correlated density distribution, drift in the measurements will tend to be accommodated by the \mathbf{v} vector rather than corrupting the \mathbf{p} vector.

To add further control over the apportioning between the two terms, the drift model can be regularised using a Tikhonov term. With this form of regularisation, the optimisation described in (5) becomes

$$\text{minimise } \left\{ (\mathbf{A}\mathbf{p} + \mathbf{B}\mathbf{v} - \mathbf{m})^2 + a((\nabla\mathbf{p} \cdot \nabla\mathbf{p}) + b(\mathbf{v} \cdot \mathbf{v})) \right\} \quad (6)$$

where a is the overall regularisation factor and b controls the relative regularisation between the density and drift models. The optimum values are determined by running a series of inversions to build

up L-curves (Hansen and O'Leary, 1993) from which the analyst can judge the best compromise between the fit to the measurements and the complexity of the model.

Results

To demonstrate the above processing procedures, we have created a test FTG data set where the acquisition pattern and noise derives from a real survey, but the signal derives from a synthetic model consisting of geological layers with the actual terrain from the survey placed on top. The noise levels assigned to the survey lines are fairly high and completely swamp the geological signal (the signal after terrain correction). Careful processing is therefore required to be able to resolve the signals of interest. Using a forward calculated geological signal makes it possible to accurately assess the error in the processed data.

The geological model was made sufficiently complex to give a realistic broad band signal similar to that experienced in real surveys. The equivalent source model was built using the terrain as the top surface and a flat horizontal plane for the bottom surface. A drift model consisting of a single linear trend was utilised for each survey line and each of the six measurement channels. An option to break down the drift along any line into more than one linear section (as shown in Figure 2) was not used since the survey lines were only 30 km long and did not have sufficient duration for complicated drift behaviour to materialise.

To solve this relatively small inversion problem, consisting of 2.7×10^5 measurements and 0.9×10^5 source prisms required 0.8 Gb of memory and less than 1 hour of computation. After solution, the inverted density model was used in isolation from the drift model to forward calculate an enhanced Gzz distribution both back at the original measurement locations and also on a level grid placed at the median of the flight height.

By differencing the known signal with these forward calculations, Figure 4 and Figure 5 show how the error in the processed Gzz varies with frequency in the survey time domain, and inverse wavelength in the space domain.

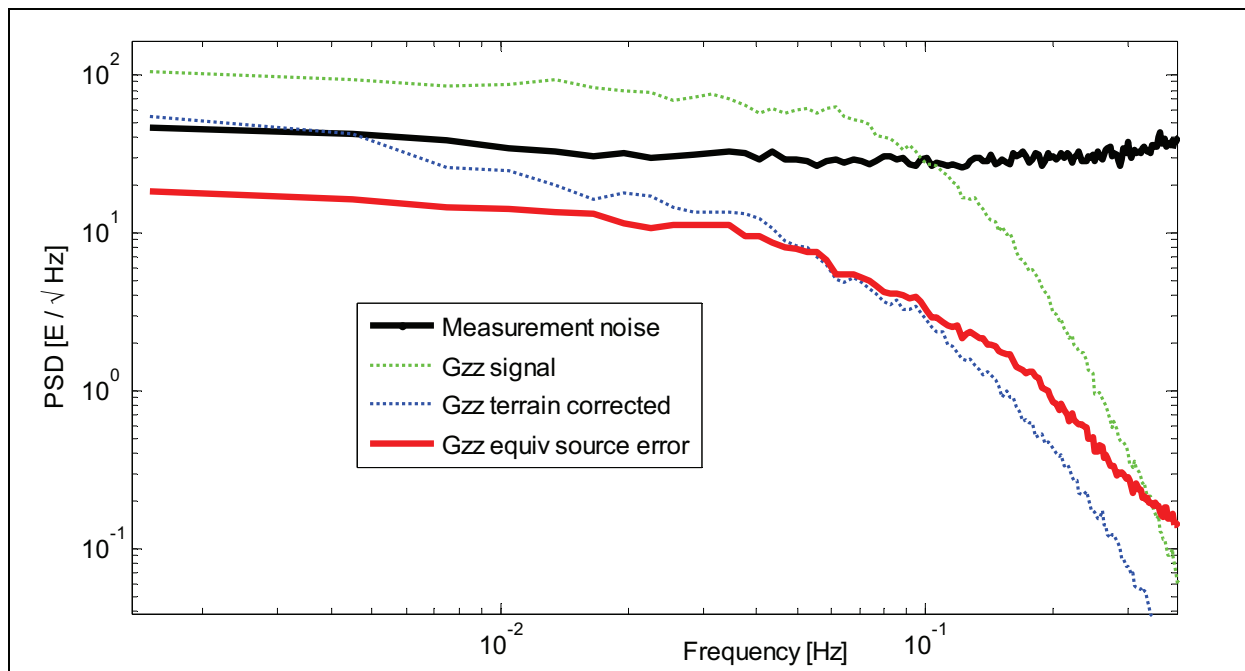


Figure 4. Average survey line time domain PSDs.

Referring to Figure 4, at low frequency (1 – 10 mHz), the error in the processed Gzz data is roughly 2.4 times less than the noise level in the original measurements. At higher frequencies, the noise reduction is greater due to the ability of the equivalent source model to correctly model the exponential upward continuation that governs the high frequency end of potential field signals. In Figure 5, the

error on Gzz crosses the geological signal at a wavelength around 0.5 – 1 km showing that for this model, anomaly wavelengths down to this level can be recovered in grids of the processed data.

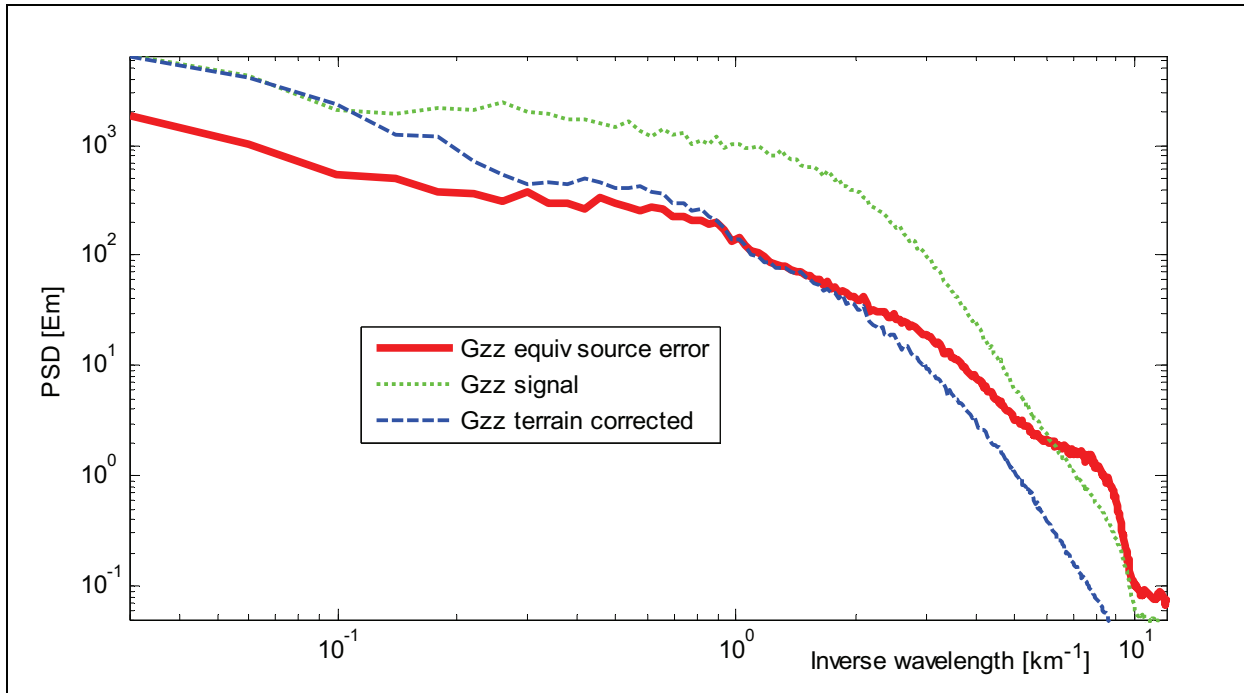


Figure 5. Gridded data radial wavenumber PSDs.

To demonstrate how well the linear drift model was able to track the low frequency noise, Figure 6 shows the fit for one of the FTG output channels over 4 survey lines. The noise series was low pass filtered to 0.01 Hz to show more clearly the low order correlated noise. One can see that the shifts in bias levels dominate and only small linear trends are apparent along these relatively short survey lines. Both are well fitted by the drift model solution.

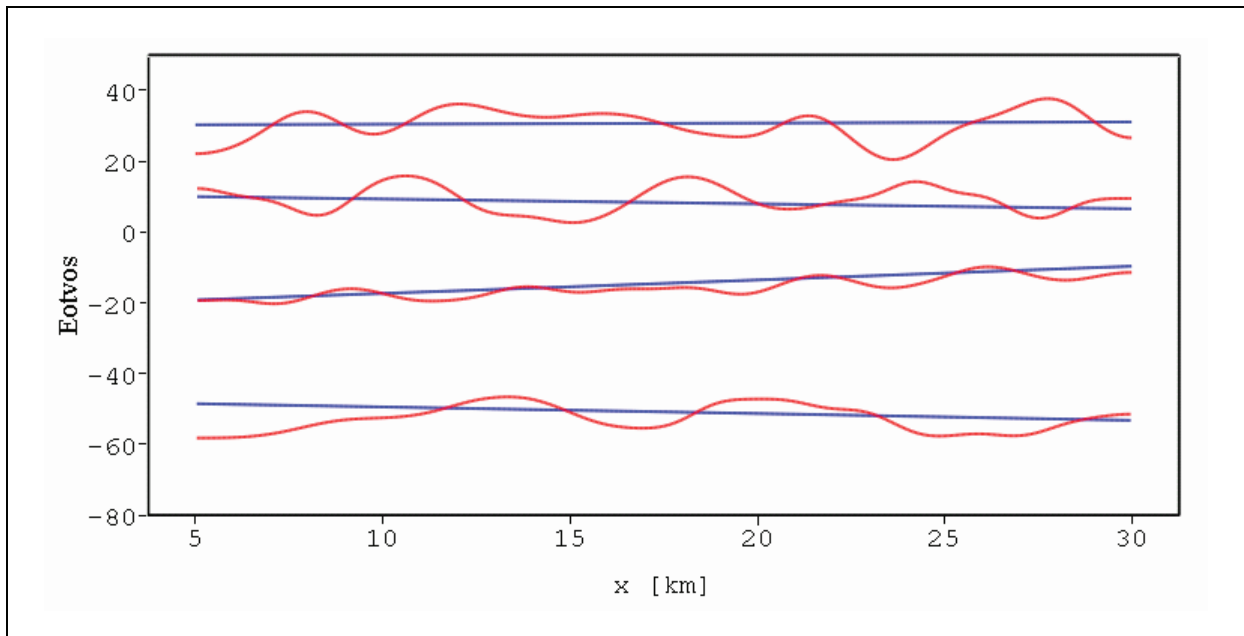


Figure 6. Red: low pass filtered noise data, Blue: linear drift model solution. Four survey lines shown.

Conclusions

The augmentation of the equivalent source inversion with a time domain drift model provides a method of reliably processing potential field data sets that contain significant bias errors or low order drift. Although a degree of low frequency noise can be removed by standard levelling procedures, these methods fail when the survey has insufficient cross-over points. The advantage of coupling a drift model with the equivalent source model is that the drift behaviour is deduced from essentially all the measurements in the survey leading to a better estimation of the drift terms, but more importantly allows surveys flown on a draped pattern to be processed.

By employing an approximation technique that groups together source elements distant from the field point in a recursive fashion, the memory requirements for the inversion are substantially reduced and consequently the solution time significantly decreased allowing commercially sized data sets to be processed on desktop personal computers. When comparing the noise levels on the FTG measurements with the error on the processed Gzz estimate, we see that for low frequencies the noise reduction is a factor of 2.4 and improves further with frequency.

References

- Barnes, G. J., 2008, Gravity survey data processing: International Patent application PCT/GB2008/050059.
- Barnes, G., Lumley, J., Houghton, P., and Gleave, R., 2010, Noise in FTG data and its comparison with conventional gravity surveys: Expanded Abstracts, EGM 2010 International Workshop - Adding new value to Electromagnetic, Gravity and Magnetic Methods for Exploration, Capri, Italy, April 11-14 2010.
- deGroot-Hedlin, C., and Constable, S., 1990, Occam's inversion to generate smooth, two-dimensional models from magnetotelluric data: *Geophysics* 55, 1613 – 1624.
- Hansen, P.C., and O'Leary, D. P., 1993, The use of the L-curve in the regularization of discrete ill-posed problems: *SIAM Journal of Scientific Computing*, 14, No.6, 1487 – 1503.
- Press, W. H., Teukolsky, S. A., Vetterling, W. T., and Flannery, B. P., 1992, *Numerical recipes in C* (2nd ed.): the art of scientific computing: Cambridge University Press.